

Preparation of Rare Earth Lu-doped TiO₂ Film by Sol-gel Method and Its Photocatalytic Degradation of Methyl Orange Under Natural Light

Ji-hui LUO *

College of Materials Science and Engineering, Yangtze Normal University, Chongqing 408100, China

crossref <http://dx.doi.org/10.5755/j02.ms.29676>

Received 30 August 2021; accepted 29 October 2021

TiO₂ can effectively degrade organic pollutants under ultraviolet radiation. Due to the large band gap of TiO₂, natural light is not suitable for catalysis, which reduces the applicability of TiO₂ materials. To use the natural light source more effectively, the sol-gel preparation process of the rare earth element Lu-doped TiO₂ thin film was studied. XRD experiment was used to analyze the crystal characteristics of Lu-doped TiO₂ film. The light absorption of Lu-doped TiO₂ film was measured by a dual-beam UV-visible spectrophotometer. The degradation effect of Lu-doped TiO₂ film on methyl orange under natural light was studied. Compared with the pure TiO₂ film, the experimental results indicate that the XRD diffraction peaks begin to shift to the left. The absorption of Lu-doped TiO₂ film intensity in the ultraviolet and visible light range is higher. Using the tangent method, the bandgap of Lu-doped TiO₂ film is estimated to be about 2.9 eV. Under natural light conditions, the characteristic peak value of the methyl orange solution decreased significantly after 72 h exposure.

Keywords: Lu-doped TiO₂ film, sol-gel, XRD, photocatalytic degradation.

1. INTRODUCTION

As early as the 1970s, it was discovered that TiO₂ has good photocatalytic properties and can be used to degrade organic pollutants [1–3]. For instance, Carey et al. [4] successfully used the photocatalytic oxidation of TiO₂ to achieve the dechlorination and detoxification of polychlorinated biphenyl compounds in water, revealing that TiO₂ has developable value in the field of environmental purification. However, the light absorption range of TiO₂ is limited to ultraviolet light and its absorption performance is poor for visible light. On the other hand, among the three main crystal forms of TiO₂, anatase is the best and brookite is the worst. With the increase of sintering temperature, TiO₂ changes from amorphous to anatase and then to rutile. Therefore, to facilitate the application of TiO₂ in the field of photocatalysis, it is necessary to inhibit the transformation from anatase to rutile (A-R) or other crystal forms as much as possible [5].

Researchers mainly modified TiO₂ films by doping various metal elements, non-metallic elements, and rare earth elements, to change the absorbable light range and physical properties of TiO₂ films. For example, in terms of metal elements, Ahadi et al. [6] doped Cu and Fe and found that the bandgap was reduced to 2.8 eV. Simeonov et al. [7] doped V element. The results showed that the conductivity of V-doped TiO₂ is higher than that of pure TiO₂. In addition, in terms of non-metallic elements, Ekemena et al. [8] doped C to study the degradation of tetracycline under visible LED. Tang et al. [9] degraded methylene blue using N-doped TiO₂ materials, etc.

In the doping of rare earth elements, La, Ce, Sm, Eu, Tb, etc. have been studied more frequently. For example,

Ren et al. [10] doped with Ce and Er. The results showed that the doped TiO₂, which is added with Er and Ce and calcined at 800 °C, can make *Staphylococcus aureus* and *Escherichia coli* have a higher resistance under visible light conditions. The antibacterial efficacy is 91.23 % and 92.8 %, respectively. Cai et al. [11] doped with Ho and found that Ho-doped TiO₂ can inhibit the A-R phase transition, improve thermal stability, and inhibit the growth of grain size. Under the same conditions, the decomposition rate of Ho-doped TiO₂ calcined at 500 °C is 3.71 times that of pure TiO₂. Zhou et al. [12] doped with Gd and also achieved remarkable results. Khade et al. [13] doped with Sm and the results showed that at a calcination temperature of 400 °C, 0.05 mol % Sm-doped TiO₂ nanoparticles have the best photocatalytic activity. In the 1 g/dm³ Sm-doped TiO₂, 96 % and 84 % of methyl orange were degraded within 120 minutes under ultraviolet and natural light irradiation, respectively. Therefore, Sm doping is effective for improving the photocatalytic activity of TiO₂ and degrading organic pollutants in water no matter under ultraviolet light or natural light. Xu et al. [14] doped rare earth elements of La³⁺, Ce³⁺, Er³⁺, Pr³⁺, Gd³⁺, Nd³⁺, Sm³⁺, and achieved the same effect.

There are also a large number of experimental studies on other rare earth elements. However, the use of rare earth Lu element for doping TiO₂ thin film has not been reported. In this paper, Lu-doped TiO₂ thin film was prepared by the sol-gel method. The optical property and photocatalysis were studied, which provided a theoretical reference for the role of TiO₂ thin film materials in improving the environment.

* Corresponding author. Tel.: +086-18210234615.
E-mail address: 20170128@yznu.cn (J.H. Luo)

2. EXPERIMENTAL

2.1. Preparation of Lu-doped TiO₂ film

At room temperature, butyl titanate, acetylacetone, and absolute ethanol were mixed in the volumes of 10 ml, 0.1 ml and 10 ml, respectively, and magnetically stirred for 30 min to prepare solution A. At the same time, deionized water and absolute ethanol were mixed in the volumes of 20 ml and 10 ml with magnetically stirring for 10 min to obtain solution B. Under magnetic stirring, solution A was slowly added to solution B, and then kept for 30 minutes. A clear and transparent sol solution can be obtained. Lutetium nitrate hexahydrate (0.6 g) was added to the sol solution. Hydrochloric acid in a volume of 0.01 ml was also added to adjust the pH value of sol solution to 1–3. All the chemical reagent manufactures are listed in Table 1.

Table 1. Chemical reagent manufactures

| Chemical reagents | Reagent manufactures |
|------------------------------|--|
| Butyl titanate | Tianjin Damao Chemical Reagent Factory |
| Hydrochloric acid | Chongqing Jiangchuan Chemical Industry |
| Acetylacetone | Shanghai Aladdin Biochemical Technology Co., Ltd |
| Absolute ethanol | |
| Lutetium nitrate hexahydrate | |

Firstly, the cover glass was selected as the glass matrix of the film. Before dipping, the cover glass was immersed in absolute ethanol and cleaned by an ultrasonic cleaning machine to remove the contaminants. Secondly, a syringe was used to evenly dip the sol solution on the surface of the cover glass. Finally, the cover glass with dipped sol solution was heated to 550 °C for 40 min using a heat treatment furnace. The main preparation process is shown in Fig. 1.

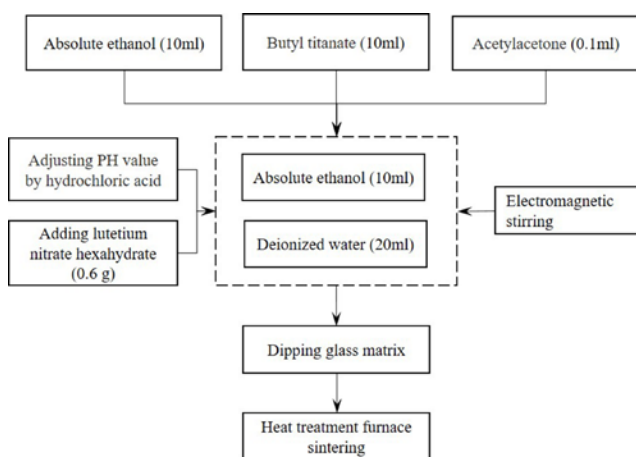


Fig. 1. Preparation process of Lu-doped TiO₂ films

Using the same method and process as above, the pure TiO₂ film was prepared for comparison in subsequent experiments.

2.2. Film thickness observation

The thickness of Lu-doped TiO₂ film was defined by XJP-6A optical microscope.

2.3. X-ray diffraction analysis

XRD-6100 X-ray diffractometer was used to detect the Lu-doped TiO₂ films. The diffraction angle range was 10° to 80° and the scanning speed was set to 10 °/min. JADE software was used to analyze the experimental diffraction pattern and qualitatively phase composition

2.4. UV-visible light analysis

The absorption spectrums of pure TiO₂ film and Lu-doped TiO₂ film are analyzed by a TU-1901 dual-beam ultraviolet-visible spectrometer. The wavelength range can be analyzed is 190 nm ~ 900 nm, the wavelength indication error is within ± 0.3 nm.

2.5. Experiment of methyl orange solution degradation

Methyl orange of 0.05 g was dissolved in 50 ml of water to prepare a methyl orange solution. Then put the prepared Lu-doped TiO₂ film into the methyl orange solution, and irradiate it under natural light for 72 hours. The light absorption experiment was performed on the illuminated solution and the original solution to analyze whether Lu-doped TiO₂ film has a degrading effect on the organic matter under natural light.

3. RESULTS AND DISCUSSION

3.1. Film thickness

The morphology of Lu-doped TiO₂ film, at 200 times magnification, is shown in Fig. 2. It can be found that the forming of thin film on the cover glass is uniform and the thickness is about 25 μm.

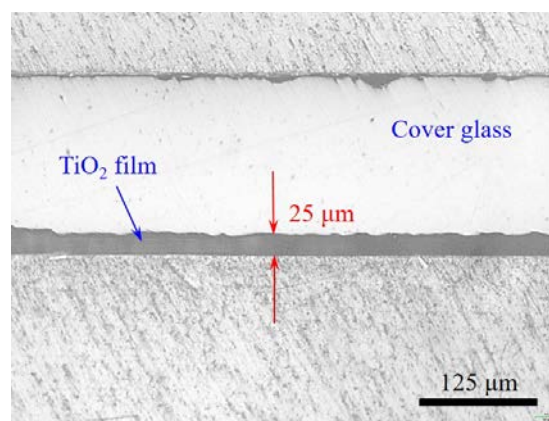


Fig. 2. Thickness morphology of Lu-doped TiO₂ film

3.2. X-ray diffraction

Fig. 3 presents the XRD experimental result. The red curve in the figure represents the XRD pattern of Lu-doped TiO₂ film. The analysis using Jade software shows that the diffraction peaks are basically consistent with the anatase TiO₂. Compared with the angle at which the diffraction peaks of standard anatase TiO₂ appear, it is found that all the peaks are shifted to the left. For instance, the experimental result of (101) surface appears the strongest peak at 25.142°, while the standard value should appear the strongest peak at 25.281°. The difference between the two is about 0.139°. The experimental result of (200) surface

appears strong peak at 47.793° , while the standard value should appear the strongest peak at 48.049° . The difference between the two is about 0.256° . The other peaks are found to be smaller than the corresponding angles of the standard anatase TiO_2 , and they move to the left as a whole.

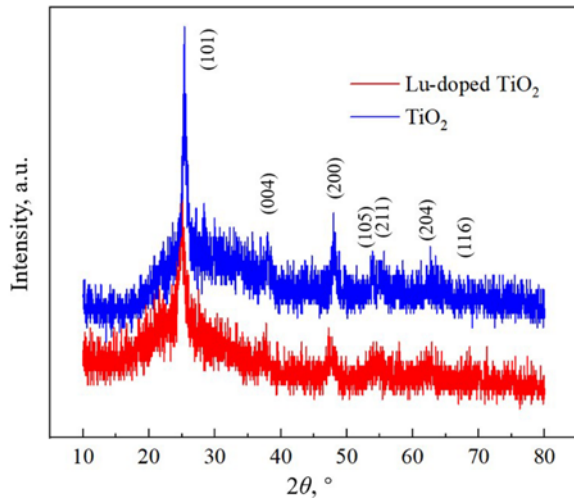


Fig. 3. XRD patterns of Lu-doped TiO_2 and pure TiO_2 films

The blue curve represents the XRD pattern of the pure TiO_2 film as shown in Fig. 3. The 2θ angles of the diffraction peaks are completely consistent with the anatase TiO_2 . It can be seen from Fig. 3 that the 2θ angles of the peaks of the Lu-doped TiO_2 film are smaller than that of the pure TiO_2 film.

Diffraction peaks moving to the left indicates that the lattice constant of anatase TiO_2 has begun to increase. After the rare earth Lu element doped TiO_2 film, because the atomic radius of the Lu element (1.73 \AA) is larger than that of the Ti atom (1.45 \AA), the lutetium element enters the TiO_2 lattice, causing the lattice constant to increase, resulting in the diffraction peaks to the left.

Previous studies have shown that TiO_2 film is brookite and the diffraction peaks of XRD will move to the right when the heat treatment temperature reaches 530°C [15]. However, after adding Lu and heating at 550°C , the crystal form of TiO_2 films does not change to brookite, indicating that the addition of Lu inhibits the occurrence of brookite.

3.3. Light absorption of Lu-doped TiO_2 film

The light absorption of Lu-doped TiO_2 film was measured by using a UV-visible spectrometer. Fig. 4 presents is the UV-visible absorption spectrum analysis results of Lu-doped TiO_2 film and pure TiO_2 film. The red curve represents Lu-doped TiO_2 film and the blue represents the result of pure TiO_2 film. It can be seen from the figure that the absorption intensity of pure TiO_2 film in the visible light range from 400 nm to 800 nm is relatively weak. In the ultraviolet wavelength range ($< 400 \text{ nm}$), absorption intensity begins to increase significantly. However, the absorption intensity of Lu-doped TiO_2 film is higher than that of pure TiO_2 film in visible and ultraviolet regions. There is also a certain absorption intensity in the visible part of 400 nm to 450 nm. Compared with pure TiO_2 film, after doping with rare earth element Lu, the absorption intensity not only increases in the ultraviolet

region but also in the visible light range.

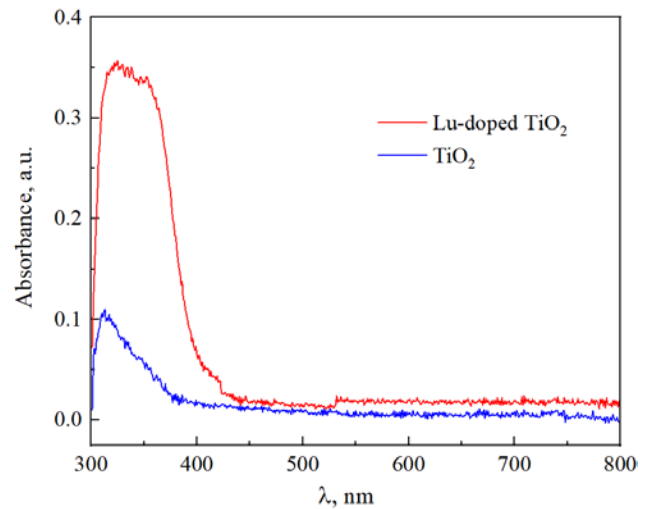


Fig. 4. The absorption spectrum of the Lu-doped TiO_2 and pure TiO_2 films

The tangent method can be used to estimate the band gap of Lu-doped TiO_2 film. From the XRD test results (Fig. 3), it can be seen that Lu-doped TiO_2 film has an anatase phase and anatase crystal structure of TiO_2 material has an indirect bandgap. The absorption spectrum wavelength λ measured by the ultraviolet-visible spectrometer is substituted into Eq. 1 for calculation [16, 17].

$$E_g = \frac{1240}{\lambda}, \quad (1)$$

where E_g is the bandgap; λ is the wavelength.

Then use the calculated result of Eq. 1 as the abscissa and use the calculated result of $(ah\nu)^{1/2}$ (α represents the absorbance) as the ordinate to draw the corresponding curve as shown in Fig. 5. The bandgap can be estimated from a plot of $(ah\nu)^{1/2}$ versus photon energy ($h\nu$). The intercept of the tangent to the curve will give an approximation of the bandgap (shown in Fig. 5) [18]. The bandgap of Lu-doped TiO_2 film is estimated to be about 2.9 eV by using the tangent method. Compared with the band gap of pure TiO_2 material (3.2 eV), the band gap begins to decrease.

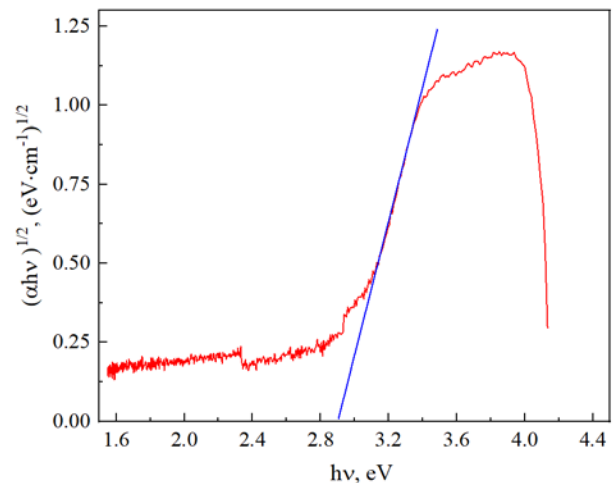


Fig. 5. Plot of $(ah\nu)^{1/2}$ versus photon energy

The above results show that the doping of element Lu can reduce the band gap of the TiO₂ film, promote the separation of photogenerated electron-hole pairs in the TiO₂ and improve the light absorption of the film.

3.4. Methyl orange degradation results

Fig. 6 is results of methyl orange solution degradation experiment. The blue solid curve in Fig. 6 represents the absorbance of untreated methyl orange solution. The blue dotted curve represents the absorbance of methyl orange solution irradiated with natural light for 72 hours. It can be seen that the characteristic peak appears near the wavelength of 462 nm. There is no significant difference between of them and the peak value is similar, indicating that there is no degradation phenomenon. However, after natural light exposure for 72 hours with Lu-doped TiO₂ films, the characteristic peak value decreases significantly as shown by the red solid curve in Fig. 6. It shows that Lu-doped film has a certain photocatalytic degradation effect on methyl orange solution under natural light.

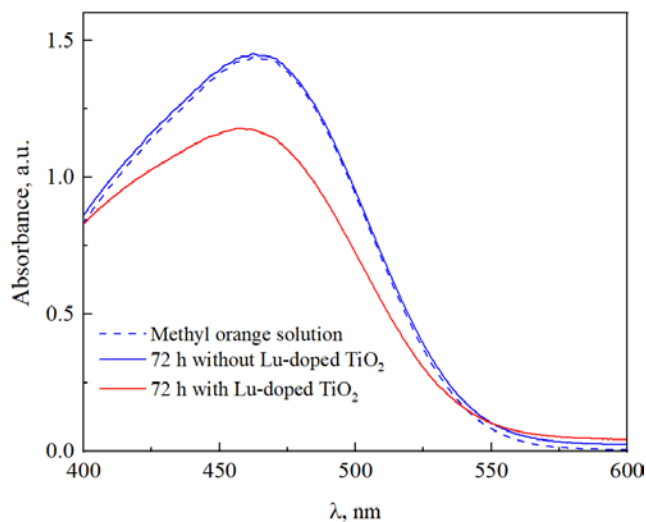


Fig. 6. The absorption spectrum of methyl orange solutions

Since the bandgap of pure TiO₂ film is 3.2 eV, according to Eq. 2, the wavelength required for the electronic transition of the pure TiO₂ film is 386 nm, which belongs to the range of ultraviolet light.

$$\lambda = \frac{hc}{E_g} \quad (2)$$

where h is Planck constant; c is the speed of light.

Through the above experiments, it is found that the band gap of Lu-doped TiO₂ is 2.9 eV. At this time, the wavelength range of light can be increased to 426 nm, which has entered the range of visible light wavelength. On the other hand, from Fig. 4, it can be found that there is a small sudden increase in the absorption of Lu-doped TiO₂ film around 426 nm. Therefore, the transition behavior of electrons can be excited under natural light and the methyl orange solution is degraded.

4. CONCLUSIONS

XRD, absorption spectrum, and methyl orange solution degradation under the natural light of Lu-doped

TiO₂ thin film, prepared by sol-gel process, were investigated. Compared with the pure TiO₂ thin film, the diffraction peaks of the Lu-doped TiO₂ thin film begin to shift to the left. In the visible range of 400 ~ 450 nm, the Lu-doped TiO₂ thin film has a certain absorption intensity. Using the tangent method, the bandgap of Lu-doped TiO₂ film is estimated to be about 2.9 eV. Lu-doped TiO₂ thin film can degrade methyl orange under natural light.

Acknowledgments

This work was financially supported by the Fuling Science and Technology Plan Project of No. FLKJ, 2019ABB2036.

REFERENCES

1. Fujishima, A., Honda, K. Electrochemical Photolysis of Water at A Semiconductor Electrode *Nature* 238 1972: pp. 37–38. <https://doi.org/10.1038/238037a0>
2. Athanasekou, C.P., Likodimos, V., Falaras, P. Recent Developments of TiO₂ Photocatalysis Involving Advanced Oxidation and Reduction Reactions in Water *Journal of Environmental Chemical Engineering* 6 (6) 2018: pp. 7386–7394. <https://doi.org/10.1016/j.jece.2018.07.026>
3. Ching, W.H., Leung, M., Leung, D.Y.C. Solar Photocatalytic Degradation of Gaseous Formaldehyde by Sol-Gel TiO₂ Thin Film for Enhancement of Indoor Air Quality *Solar Energy* 77 (2) 2004: pp. 129–135. <https://doi.org/10.1016/j.solener.2004.05.012>
4. Carey, J.H., Lawrence, J., Tosine, H.M. Photodechlorination of PCBs in The Presence of TiO₂ in Aqueous Suspensions *Bulletin of Environmental Contamination and Toxicology* 16 (6) 1976: pp. 697–701. <https://doi.org/10.1007/BF01685575>
5. Nolan, N.T., Seery, M.K., Pillai, S.C. Spectroscopic Investigation of the Anatase-to-Rutile Transformation of Sol-Gel-Synthesized TiO₂ Photocatalysts *Journal of Physical Chemistry C* 113 (36) 2009: pp. 16151–16157. <https://doi.org/10.1021/jp904358g>
6. Ahadi, S., Moalej, N.S., Sheibani, S. Characteristics and Photocatalytic Behavior of Fe and Cu Doped TiO₂ Prepared by Combined Sol-Gel and Mechanical Alloying *Solid State Sciences* 96 2019: pp. 105975. <https://doi.org/10.1016/j.solidstatesciences.2019.105975>
7. Simeonov, S., Szekeres, A., Covei, M., Spassov, D., Zaharescu, M. Inter-trap Tunneling in Vanadium Doped TiO₂ Sol-Gel Films *Materials Research Bulletin* 127 2020: pp. 110854. <https://doi.org/10.1016/j.materresbull.2020.110854>
8. Ekemena, O.O., Ofomaja, A.E. Facile Microwave Synthesis of Pine Cone Derived C-doped TiO₂ for The Photodegradation of Tetracycline Hydrochloride under Visible-LED Light *Journal of Environmental Management* 223 2018: pp. 860–867. <https://doi.org/10.1016/j.jenvman.2018.07.003>
9. Tang, X., Wang, Z., Huang, W., Jing, Q., Liu, N. Construction of N-doped TiO₂/MoS₂ Heterojunction with Synergistic Effect for Enhanced Visible Photodegradation Activity *Materials Research Bulletin* 105 2018: pp. 126–132. <https://doi.org/10.1016/j.materresbull.2018.04.046>

10. **Ren, Y., Han, Y., Li, Z., Liu, X., Wu, S.** Ce and Er Co-doped TiO₂ for Rapid Bacteria-killing Using Visible Light *Bioactive Materials* 5 2020: pp. 201–209.
<https://doi.org/10.1016/j.bioactmat.2020.02.005>
11. **Cai, H., Liu, G., Lu, W., Li, X., Yu, L., Li, D.** Effect of Ho-doping on Photocatalytic Activity of Nanosized TiO₂ Catalyst *Journal of Rare Earths* 26 2008: pp. 71–75.
[https://doi.org/10.1016/S1002-0721\(08\)60040-X](https://doi.org/10.1016/S1002-0721(08)60040-X)
12. **Zhou, Y., Zhang, S., Zhu, Z., Li, Y.** Preparation and Photocatalytic Activity of Gd-doped TiO₂ Nanofiber *Journal of Central South University of Technology* 12 (6) 2005: pp. 657–661.
<https://doi.org/10.1007/s11771-005-0064-3>
13. **Khade, G.V., Suwarnkar, M.B., Gavade, N.L., Garadkar, K.M.** Sol-Gel Microwave Assisted Synthesis of Sm-doped TiO₂ Nanoparticles and Their Photocatalytic Activity for the Degradation of Methyl Orange under Sunlight *Journal of Materials: Materials in Electronics* 27 (6) 2016: pp. 6425–6432.
<https://doi.org/10.1007/s10854-016-4581-7>
14. **Xu, A., Gao, Y., Liu, H.** The Preparation, Characterization, and their Photocatalytic Activities of Rare-Earth-Doped TiO₂ Nanoparticles *Journal of Catalysis* 207 (2) 2002: pp. 151–157.
<https://doi.org/10.1006/jcat.2002.3539>
15. **Luo, J., Wen, Q., Liu, S., Liu, T., Wei, S., Yang, R.** Preparation of TiO₂ Thin Films by Sol-Gel Method and Analysis of its Transmittance Based on Computer Image Processing *Key Engineering Materials* 842 2020: pp. 121–126.
<https://doi.org/10.4028/www.scientific.net/KEM.842.121>
16. **Ji, P., Zhang, J., Chen, F., Anpo, M.** Ordered Mesoporous CeO₂ Synthesized by Nanocasting from Cubic Ia3d Mesoporous MCM-48 Silica: Formation, Characterization and Photocatalytic Activity *Journal of Physical Chemistry C* 112 2008: pp. 17809–17813.
<https://doi.org/10.1021/jp8054087>
17. **Zhao, Y., Li, C., Liu, X., Gu, F., Jiang, H., Shao, W., Zhang, L., He, Y.** Synthesis and Optical Properties of TiO₂ Nanoparticles *Materials Letters* 61 2007: pp. 79–83.
<https://doi.org/10.1016/j.matlet.2006.04.010>
18. **Hao, J., Wang, Y., Tong, X., Jin, G., Guo, X.** SiC Nanomaterials with Different Morphologies for Photocatalytic Hydrogen Production under Visible Light Irradiation *Catalysis Today* 212 2013: pp. 220–224.
<https://doi.org/10.1016/j.cattod.2012.09.023>



© Luo 2022 Open Access This article is distributed under the terms of the Creative Commons Attribution 4.0 International License (<http://creativecommons.org/licenses/by/4.0/>), which permits unrestricted use, distribution, and reproduction in any medium, provided you give appropriate credit to the original author(s) and the source, provide a link to the Creative Commons license, and indicate if changes were made.